I&EC research
Industrial & Engineering Chemistry Research

Thermodynamics, Transport, and Fluid Mechanics

Strategy Combining Free Volume Theory and Fragment Contribution Corresponding State Method for Predicting Viscosities of Ionic Liquids

Wenhui Tu, Shaojuan Zeng, Xiaochun Zhang, Xuezhong He, Lei Liu, Suojiang Zhang, and Xiangping Zhang

Ind. Eng. Chem. Res., **Just Accepted Manuscript** • DOI: 10.1021/acs.iecr.8b06255 • Publication Date (Web): 18 Mar 2019

Strategy Combining Free Volume Theory and Fragment Contribution Corresponding State Method for Predicting Viscosities of Ionic Liquids

Wenhui Tu,[a,b] Shaojuan Zeng,[*,a] Xiaochun Zhang,[a] Xuezhong He,[c] Lei Liu,[a] Suojiang Zhang,[a,b] Xiangping Zhang[*,a,b,d]

[a] Key Laboratory of Green Process and Engineering, State Key Laboratory of Multiphase Complex Systems, Beijing Key Laboratory of Ionic Liquids Clean Process, Institute of Process Engineering, Chinese Academy of Sciences, Beijing 100190, China.

[b] School of Chemistry and Chemical Engineering, University of Chinese Academy of Sciences, Beijing 100049, China.

[c] Department of Chemical Engineering, Norwegian University of Science and Technology, NO-7491, Trondheim, Norway.

[d] Dalian National Laboratory for Clean Energy, Dalian 116023, China.

Abstract

In this study, we proposed a strategy that combines the fragment contribution corresponding states (FCCS) and free volume theory (FVT) method, namely FCCS-FVT, to calculate the viscosities of ILs covering a wide range of temperatures and pressures. In the method, the FCCS model was used to calculate the critical properties and densities of ILs, and then based on those values, the FVT model was applied to calculate the viscosities of ILs. The results indicated that the FCCS-FVT method shows high accuracy with 6.6% in average absolute relative deviation of total 2138 data points (25 ILs), which covers a wide range of temperatures (258.15–573 K) and pressures (0.06–300 MPa). Moreover, it is more convenient for the FCCS-FVT method to be applied for quick and accurate calculation of viscosities of ILs because it needs only three adjustable parameters.

Keywords: FCCS-FVT, ionic liquids, viscosity, prediction, model

1. INTRODUCTION

As an environment friendly solvents, ionic liquids (ILs) have attracted intensive attention from the researchers and show high potential to replace traditional solvents in many industrial processes.[1,2] However, their viscosities are much higher than conventional solvents, and typically lie in a wide range from 2.2 mPa·s to 21645.1 mPa·s at 298.15 K and at the atmospheric pressure.[3,4] In addition, it is reported that the number of potential ILs is as high as 10^{18}.[5] Thus, it is necessary but great challenge to develop a model to predict the viscosities of ILs. It is well known that viscosity is one of the important properties of ILs, which strongly affects the mass- and heat-transfer rate and transport behaviors.[6] The viscosities are dramatically influenced by the operational conditions, especially temperatures and pressures. The whole pressure−temperature−viscosity ($P\eta T$) behaviors of ILs can be used to determine the feasible operation conditions for a real chemical process, such as fluids pumping and stirring.[7] Generally, the available experimental viscosities of ILs that can be used to guide industrial applications are far from adequate. Therefore, developing reliable and efficient models to predict viscosities of ILs at different temperatures and pressures are critical for industrial applications of ILs.

To predict viscosities of ILs, some models are reported in the literature.[8-14] Most of them are only applicable for predicting viscosities of ILs at different temperatures while the pressure is a constant (e.g., 1 atm). To the best of our knowledge, there are just a few models for calculating viscosities of ILs are valid considering both different temperatures and pressures. So far, the framework that simultaneously combines transport and thermodynamic models is the most popular one being applied to describe the $P\eta T$ behaviors of ILs.[15-19] In this framework, the thermodynamic models provide the necessary thermodynamic properties of ILs as input for the theoretical models to calculate viscosities. Among them, the friction theory (FT)[20] and the free volume theory (FVT)[21] are adopted to combine with different types of equations of state (EoS). In Haghbakhsh's study, the FVT and FT models were combined with four EoSs (i.e., Peng−Robinson (PR), Soave−Redlich−Kwong (SRK), cubic plus association (CPA),

and perturbed-chain statistical associating fluid theory (PC-SAFT)), respectively, to model the viscosities of ILs.[15] Overall, FT model shows higher accuracy than FVT model mainly due to the former requires more adjustable parameters. The parameters for FT and FVT are 12 and 3, respectively. Among these eight models, FT+PC-SAFT model has the minimum average absolute relative deviation (*AARD*) of 2.37% and FVT+SRK has the maximum *AARD* of 18.7%, and the *AARD* could decrease to 3.75% when FVT is coupled with PC-SAFT. The reliability of FVT and FT models coupled with different version of SAFT models have been further proven to describe the $P\eta T$ behaviors of ILs.[16-18] However, the different versions of SAFT models are relatively complex and difficult to be implemented. Therefore, it is valuable to develop a simpler model to calculate the viscosities of ILs at different temperatures and pressures with satisfactory accuracy.

In our previous work, the fragment contribution corresponding states (FCCS) method was proposed to predict the critical properties of ILs and the physicochemical properties (e.g., density, surface tension, heat capacity, and thermal conductivity) of ILs.[22] The results indicated that the FCCS method shows high accuracy with an *AARD* of less than 4%. For the density, the overall *AARD* is less than 2.1% of the whole data set (5179 data points) by using Riedel equation. On the other hand, the FVT model needs only 3 parameters, which is simpler than FT model. In addition, it has been proved that FVT model is capable to predict the viscosities of ILs by combining suitable thermodynamic models, for example, Abolala et al. combined FVT model and SAFT-VR-Mie model to predict the viscosities of ILs with an *AARD* of 3.81% for 11 ILs.[18] Therefore, combining FCCS and FVT models would be a successful strategy to efficiently calculate the viscosities of ILs at different temperatures and pressures. Furthermore, their combination will enable the model to be applied to process simulations and integrations, and numerical simulations of bubble behavior and mass transfer.[23]

In this study, we develop a method to predict the viscosities of ILs by combining FCCS and FVT models, namely FCCS-FVT. The development procedure is as follows: First, we collect the experimental viscosities of 25 ILs covering a wide range of

temperatures and pressures from literature; Second, FCCS method is used to calculate the critical properties and densities of ILs as input for FVT model; Finally, the parameters of FVT are optimized with experimental data. Then viscosities of ILs are calculated by FCCS-FVT method, and accuracy is discussed and compared with previous models.

2. METHODOLOGY

2.1. Free volume theory.

The free volume theory (FVT) was proposed by Allal et al.[21] The viscosity is divided into two parts, the viscosity of dilute gas, η_0, and the residual friction viscosity term, η_f.

$$\eta = \eta_0 + \eta_f \tag{1}$$

The viscosity of the dilute gas is calculated by Eq. (2).[15,16]

$$\eta_0 = 40.785 \frac{\sqrt{M_W T}}{V_c^{2/3} \Omega^*} F_c \tag{2}$$

Where M_W is the molecular weight and V_c is the critical volume. The parameters of Ω^* and F_c are calculated by Eqs. (3)–(5).[15,16]

$$\begin{aligned}\Omega^* = &\frac{1.16145}{T^{*0.14874}} + \frac{0.52487}{\exp(0.77320T^*)} + \frac{2.16178}{\exp(2.43787T^*)} \\ &-6.435\times10^{-4} T^{*0.14874} \sin\left(18.0323T^{*-0.76830} - 7.27371\right)\end{aligned} \tag{3}$$

With

$$T^* = \frac{1.2593T}{T_c} \tag{4}$$

$$F_c = 1 - 0.2756\omega + 0.059035\mu_r^4 + k \tag{5}$$

Where k, μ_r and ω are the associating bond effect parameter, dimensionless dipole moment, and acentric factor, respectively. μ_r is expressed as

$$\mu_r = 131.3\mu / \left(V_c T_c\right)^{0.5} \tag{6}$$

Where T_c and μ are the critical temperature and dipole moment, respectively.

The residual term for the FVT is expressed by the following equation:[15,16,21]

$$\eta_f = \frac{\rho l\left(\alpha\rho + \frac{PM_W}{\rho}\right)}{\sqrt{3RTM_W}} \exp\left[B\left(\frac{\alpha\rho + \frac{PM_W}{\rho}}{RT}\right)^{3/2}\right] \tag{7}$$

Where ρ, M_W, R, T, P and B are density, molecular weight, universal gas constant, temperature, pressure, and characteristic of the molecule, respectively. l is a parameter homogeneous with length. The parameter α is a barrier energy. FCCS method is used as auxiliary equations with this model for calculating densities, the critical properties and acentric factor of ILs (see section 2.2). The parameters (l, α, and B) are optimized based on experimental data with Eq. (8) as the objective function.

$$OF. = \frac{1}{N_p}\sum_{i}^{N_p}\left(\frac{\eta_i^{\exp} - \eta_i^{cal}}{\eta_i^{\exp}}\right)^2 \tag{8}$$

Where $\eta_i^{\exp}$ and η_i^{cal} are the experimental and calculated viscosities, respectively, and N_p is the total number of data used in the optimization.

To calculate viscosities of ILs with the FVT model, the critical properties, acentric factors and densities of ILs are necessary, which can be calculated by FCCS method (see section 2.2). The critical properties and acentric factors of the investigated ILs are summarized in Table S26. In addition, the correction factors k and μ are also required for calculating η_0. Shen et al.[16] assumed the k of ILs to be the same as that for ethanol (k = 0.174823), and assumed ILs' dipole moment μ to be the same as that for methanol (μ = 1.7 D). Later, the same solution was adopted in the study of Haghbakhsh et al.[15] These approximations are accurate enough since the contribution of the dilute gas viscosity to the total viscosity is negligible. Therefore, the same approximations have been employed in our study.

2.2. FCCS method.

2.2.1. The ionic fragment for FCCS method.

The ionic fragments used in current study are taken from our previous work.[22] Each IL is composed of three parts: cation fragment, anion fragment, and substituent fragment attached to cations or anions. The cation and anion fragments represent the

charge center of cation and anion, respectively. The H atoms attached to a ring are defined into a substituent fragment, named –H(ring). The typical cation and anion fragments are shown in Figure 1, and an exemplary fragment assignment is shown in Figure 2 for a representative IL, namely 1-butyl-3-methylimidazolium bis[(trifluoromethyl)sulfonyl]imide ([BMIm][Tf_2N]). The complete set of 46 fragments, including 7 cation fragments, 18 anion fragments, and 21 substituent fragments, and their increments for T_b and critical properties are presented in our previous work.[22]

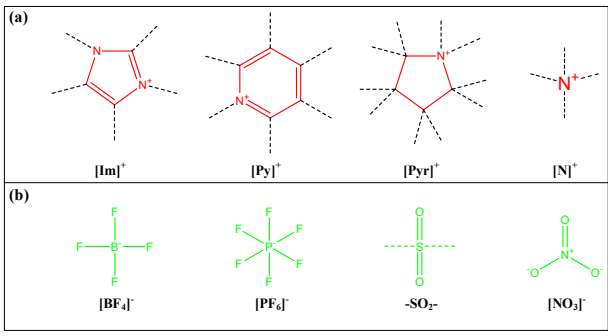

Figure 1. Typical fragments of ILs. (a) Cation fragments, (b) Anion fragments.

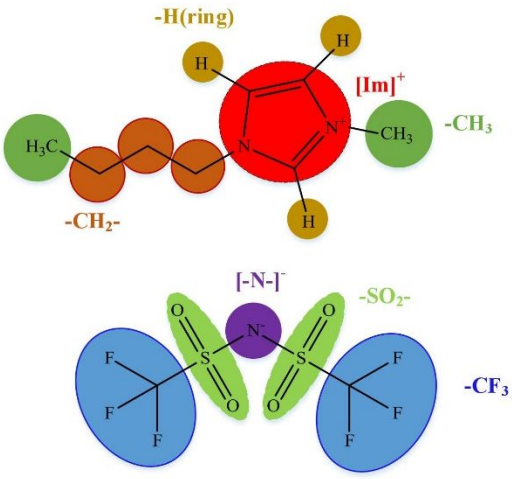

Figure 2. An exemplary fragment assignment of [BMIm][Tf_2N] in terms of the proposed FCCS method: 1 × $[Im]^+$, 3 × –H(ring), 2 × –CH_3, 3 × –CH_2–, 2 × –SO_2–, 1 × $[–N–]^–$, 2 × –CF_3.

2.2.2. Critical properties and densities calculations.

As shown in section 2.1, the critical properties and densities of ILs are required for FVT model. These properties can be calculated with FCCS method proposed in our previous work.[22] It has been shown that the Riedel corresponding states equation[24] represents the highest accuracy to calculate the densities of ILs. Therefore, in this study,

the Riedel equation (Eq. (9)) is adopted to calculate the densities of ILs. The normal boiling temperature (T_b) and the critical properties (i.e., critical temperature (T_c), critical pressure (P_c), critical volume (V_c) and acentric factor (ω)) of ILs are calculated by Eqs. (10)–(14).[22]

$$\rho = \frac{M_W}{V_c}\left[1 + 0.85\left(1 - T_r\right) + \left(1.6916 + 0.984\omega\right)\left(1 - T_r\right)^{1/3}\right] \tag{9}$$

$$T_b = 198.2 + \sum_i n_i \Delta T_{b,i} \tag{10}$$

$$T_c = \frac{T_b}{0.5703 + 1.0121\sum_i n_i \Delta T_{c,i} - \left(\sum_i n_i \Delta T_{c,i}\right)^2} \tag{11}$$

$$P_c = \frac{M_W}{\left(0.34 + \sum_i n_i \Delta T_{c,i}\right)^2} \tag{12}$$

$$V_c = 28.8946 + 14.75246\sum_i n_i \Delta V_{c,i} + \frac{6.03853}{\sum_i n_i \Delta V_{c,i}} \tag{13}$$

$$\omega = \frac{T_b}{0.7\left(T_c - T_b\right)}\log\left(\frac{P_c}{P_b}\right) - \frac{T_c}{\left(T_c - T_b\right)}\log\left(\frac{P_c}{P_b}\right) + \log\left(\frac{P_c}{P_b}\right) - 1 \tag{14}$$

Where n_i represents the number of fragment i that appears in an IL; $\Delta T_{b,i}$, $\Delta T_{c,i}$, $\Delta P_{c,i}$ and $\Delta V_{c,i}$ denote the increments of fragment i for the normal boiling temperature, critical temperature, critical pressure and critical volume, respectively; P_b is the atmospheric pressure, setting up 100 kPa in this study; T_r is the reduced temperature defined as $T_r = T/T_c$.

2.3. Model evaluation.

Models are often evaluated by several metrics. Squared correlation coefficient, R^2, which gives a fraction of explained variance for a data set, is utilized to evaluate the model's fit performance. Relative deviation (*RD*), absolute relative deviation (*ARD*), average absolute relative deviation (*AARD*) and mean square error (*MSE*) are used to measure the model's predictive effectiveness. These metrics are defined by following equations:

$$R^2 = \frac{\sum_{i=1}^{N_p}\left(y_i^{\exp} - y_m\right)^2 - \sum_{i=1}^{N_p}\left(y_i^{\exp} - y_i^{cal}\right)^2}{\sum_{i=1}^{N_p}\left(y_i^{\exp} - y_m\right)^2} \tag{15}$$

$$RD_i\left(\%\right) = 100 \times \frac{y_i^{cal} - y_i^{\exp}}{y_i^{\exp}} \tag{16}$$

$$ARD_i\left(\%\right) = 100 \times \left|\frac{y_i^{cal} - y_i^{\exp}}{y_i^{\exp}}\right| \tag{17}$$

$$AARD\left(\%\right) = 100 \times \sum_{i=1}^{N_p}\left|\frac{y_i^{cal} - y_i^{\exp}}{y_i^{\exp}}\right| \Big/ N_p \tag{18}$$

$$MSE = \sqrt{\sum_{i=1}^{N_p}\left(y_i^{cal} - y_i^{\exp}\right)^2 \Big/ N_p} \tag{19}$$

Here y donates the property of viscosity, y_m is the mean of experimental viscosities. The superscripts '*cal*' and '*exp*' represent calculated and experimental value, respectively, and N_p is the total number of data for a system or whole data set.

2.4. Data set.

In the present work, all experimental data are taken from IL Thermo Database.[25] The viscosity values of ILs may be significantly different due to different authors, measuring methods, and the purity of ILs. The aim of this work is to study the $P\eta T$ behaviors of ILs at different temperatures and pressures. Therefore, the viscosities measured at different temperatures and pressures are adopted. In the case that the viscosities measured at the same operation conditions (e.g., temperatures and pressures) by different researchers, the outliers are discarded firstly and then the data of higher purity ILs is accepted. The pressures are assigned to 100 kPa for the data points measured at "ambient pressure" or at unknown pressures. Considering the available application of the FCCS method, a total of 2138 experimental viscosity data points of 25 ILs are collected mainly based on alkyl-substituted cations, including imidazolium $[Im]^+$, pyridinium $[Py]^+$, pyrrolidinium $[Pyr]^+$, and anions, containing tetrafluoroborate $[BF_4]^-$, hexafluorophosphate $[PF_6]^-$, bis[(trifluoromethyl)sulfonyl]imide $[Tf_2N]^-$, dicyanamide $[Dca]^-$, methylsulfate $[MeSO_4]^-$, ethyl sulfate $[EtSO_4]^-$, and

trifluoromethanesulfonate $[CF_3SO_3]^-$. The summary of collected viscosity data points of 25 ILs are listed in Table 1. The details of all data are also provided in ESI from Table S1 to Table S25.

To optimize the parameters of the FVT model, about half of the data for each IL were randomly selected as training set, and the remaining data were used as testing set to test the parameters of FVT model. The process to determine the training set and test set was as follows: Firstly, a vector of random (V_r) was generated using *RAND* function in Excel for the experimental data of each IL. Secondly, the elements of V_r were marked with ascending order until reaches the needed number (half of the number of data points for each IL). Thirdly, the experimental data which had the same indexes as marked elements were defined as training set while the rest data were used as test set.

Table 1. Summary of selected literature data for the viscosities of ILs

ILs	N_p	T range (K)	P range (MPa)	η range (mPa·s)	Refs.
[(2,3-M)BIm][Tf_2N]	45	273.15–373.15	0.1–150	8.81–519	26, 27
[BMIm][BF_4]	192	273.15–388.04	0.1–300	5.8–875	28-34
[BMIm][PF_6]	175	273.15–413.2	0.1–249.3	7.1–2700	28, 30, 32, 34-40
[BMIm][Tf_2N]	115	273.15–573	0.1–298.9	1.13–280	28, 30, 32, 41-43
[BMPyr][CF_3SO_3]	74	283.15–373.15	0.1–150	12.95–738	27, 44
[BMPyr][Tf_2N]	101	273.15–373.15	0.1–150	8.45–1185	27, 45, 46
[BPy][BF_4]	73	278.15–353.15	0.06–65.85	15.84–1057	7, 47-49
[BPy][CF_3SO_3]	46	298.15–338.15	0.1–64.88	24.62–175	7, 47
[C_{10}MIm][Tf_2N]	49	278–393	0.1–122.57	6.8–460	35, 43
[C_3Py][BF_4]	71	278.15–338.15	0.1–65.91	21.97–616	7, 50
[C_4(2-M)Py][BF_4]	61	288.15–338.15	0.1–65.69	38.2–860	7, 51
[C_4(3-M)Py][BF_4]	73	278.15–343	0.07–65.05	23–1281	7, 52, 53
[C_4(3-M)Py][Dca]	81	278.15–348.15	0.1–61.47	7.22–107.9	7, 54, 55
[C_4(4-M)Py][BF_4]	69	278.15–373.15	0.1–64.96	10.5–1689	7, 52, 55, 56
[C_6MIm][BF_4]	122	283.15–368.15	0.1–121.81	13.92–819	33, 35, 57-60
[C_6MIm][PF_6]	103	273.15–368.15	0.1–238.5	17.9–3924	35, 41, 61, 62
[C_6MIm][Tf_2N]	102	258.15–433.15	0.1–124	2.86–942	35, 43, 63-65
[C_8(3-M)Py][BF_4]	45	283.15–333.15	0.08–64.8	61.4–2341	7
[C_8MIm][BF_4]	150	273.15–363.15	0.1–224.2	21.6–2291	33, 60, 66, 67
[C_8MIm][PF_6]	66	278.15–363.15	0.1–175.9	31.49–6410	61, 66, 68
[DMIm][$MeSO_4$]	66	293.15–438.15	0.1–70	3.5–92.8	69-71
[EMIm][BF_4]	74	269.15–363.15	0.1–14.5	7.225–145	31, 33, 72
[EMIm][$EtSO_4$]	24	313.15–363.15	10–150	13.2–154	46
[EMIm][Tf_2N]	113	263.15–393.15	0.1–125.53	3.7–175.1	28, 30, 35, 43, 57, 72-74

[(MoE)Mpyr][Tf_2N]	48	258.15–373.15	0.1–150	7.26–620	27, 46

*: The full names of ionic liquids can be found in Appendix A.

3. RESULTS AND DISCUSSION

3.1. Model evaluation.

In the FVT model, only three adjustable parameters (i.e., l, α and B) are needed to be optimized using the experimental data, which is achieved by employing Eq. (8) as objective function for each IL. The optimized parameters are summarized in Table S26.

With the optimized parameters, the viscosities of ILs are calculated at the whole pressures and temperatures as listed in Table 1. The calculated viscosities, experimental values, relative deviations and absolute relative deviations of each IL are summarized in Table S1−S25. Figure 3(a) shows the comparison between experimental and calculated viscosities using the FCCS-FVT model. The results show that most of the data points distribute tightly close to the diagonal of $y=x$, and the squared correlation coefficient, R^2, for the training, test and entire data set are 0.973, 0.957, and 0.965, respectively, indicating the calculated viscosities are consistent well with experimental values. The *AARD*, quantifies the magnitude of the scatter for the training, test and entire data set are 6.4%, 6.8%, and 6.6%, respectively. This indicates that the scatter of the data set is small.

The relative deviations for all experimental data are depicted in Figure 3(b). The results show that most of the data are distributed in the range where the relative deviations are less than ±10%. The *ARD* distribution and the corresponding percentage are shown in Figure 3(c). It shows that 50.4% of entire data set lie in the range of 0-5% and 81.2% of entire data set lie in the range of 0-10%, which cover the *AARD* of the whole data set. The number of data points with an *ARD* of less than 20% covers 95.0% of the whole data set. There are only three data points with *ARD* of >50%. In summary, the high R^2 (> 0.95) and small *AARD* (< 10%) imply that the FCCS-FVT method is rather accurate for prediction of the viscosities of ILs in a wide range of temperatures and pressures.

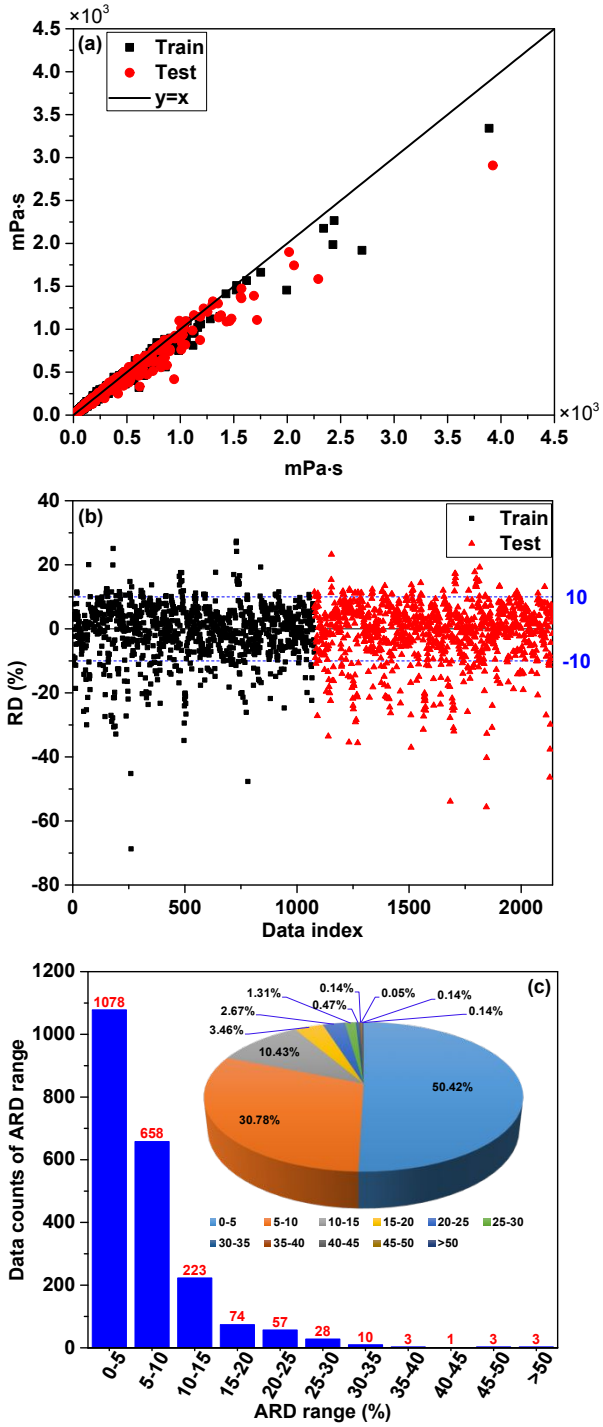

Figure 3. The comparisons between experimental and calculated viscosities of ILs from FCCS-FVT. (a) Calculated versus experimental viscosities, (b) Relative deviations versus data index, (c) Data number and percent of *ARD* value in different deviation ranges. (The number on the top of a bar represents the number of *ARD* that lies in the corresponding deviation range)

3.2. Deviation analysis for FCCS-FVT model.

The *MSE*, *AARD* and R^2 of each IL for training, test and whole data set are summarized in Table S27. The results show that [C_4(2-M)Py][BF_4] has relative high *AARD* of 13.3% with an acceptable R^2 of 0.875. [C_6MIm][Tf_2N] and [(MoE)Mpyr][Tf_2N] have relative small R^2 which are 0.740 and 0.799, respectively, and the corresponding *AARDs* for these two ILs are 9.8% and 8.2%, respectively. Figure 4(a)–(c) depict the calculated viscosities using the FCCS-FVT method versus the corresponding experimental values of [C_6MIm][Tf_2N], [(MoE)Mpyr][Tf_2N] and [C_4(2-M)Py][BF_4], respectively. Note that there are several data points show large deviations for [C_6MIm][Tf_2N] and [(MoE)Mpyr][Tf_2N]. After reviewing the data details (see Table S17 and Table S25), it is found that these data lie in low temperatures (< 298.15 K, the data items have been marked in red color). When excluding these data points, the *AARD*s for [C_6MIm][Tf_2N] and [(MoE)Mpyr][Tf_2N] decrease to smaller values (8.3% and 6.2%), and the corresponding R^2 increase to higher values (0.977 and 0.964). Unlike forward mentioned two ILs, many data points of [C_4(2-M)Py][BF_4] have larger *ARD* of >10%. However, most of them distribute on both side of the diagonal of $y=x$. The deviations are not as significant as the data with large deviation of [C_6MIm][Tf_2N] and [(MoE)Mpyr][Tf_2N]. The detailed data of [C_4(2-M)Py][BF_4] are given in Table S11, and the results show that its maximum *ARD* is 34.9%.

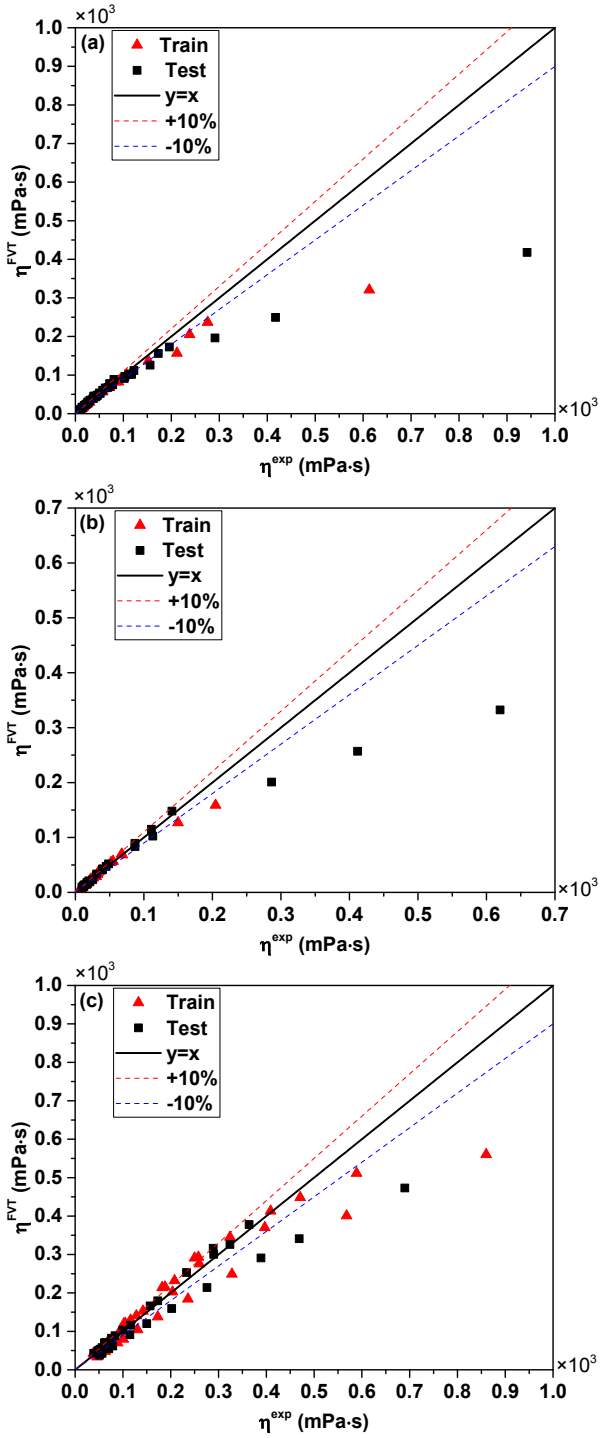

Figure 4. Calculated versus experimental viscosities using the FCCS-FVT model for ILs. (a) $[C_6MIm][Tf_2N]$, (b) $[(MoE)Mpyr][Tf_2N]$, (c) $[C_4(2\text{-}M)Py][BF_4]$.

3.3. The contribution of dilute gas viscosity.

As described in section 2.1, the FVT model has more complicated mathematical expressions for calculating η_0 than those for calculating η_f. As shown in Table S1–S25, the order of magnitude of dilute gas viscosities is significantly lower than that of total viscosities. The percentages of dilute gas viscosities with respect to total viscosities (η_0/η^{FVT}, %), and the *MSE*, *RD*, *AARD* and R^2 for the FVT model ignoring the dilute gas viscosity contributions are calculated (see Table S27). The average of η_0/η^{FVT} is 0.02% for the whole data set and the new statistical quantities (i.e., *MSE*, *RD*, *AARD* and R^2) are almost identical to the data when dilute gas viscosities are included. These results indicate that the contribution of dilute gas viscosities to the total viscosities is negligible. The maximum η_0/η^{FVT} is 3.25% for [BMIm][Tf_2N] at 573.0 K and 100 kPa. The experimental and calculated viscosities of [BMIm][Tf_2N] at 100 kPa and at different temperatures are plotted in Figure 5. It is shown that the curves of η_f and η^{FVT} are almost overlap and agree well with experimental data. Moreover, it can be seen that η_f decreases dramatically with the increase of temperature, while η_0 almost remains a constant. Therefore, for condensed fluid with high viscosity, such as ILs, the dilute gas viscosity item in the FVT model can be ignored. As a result, the mathematical expression of the FVT model becomes more simplified, and easier to be implemented.

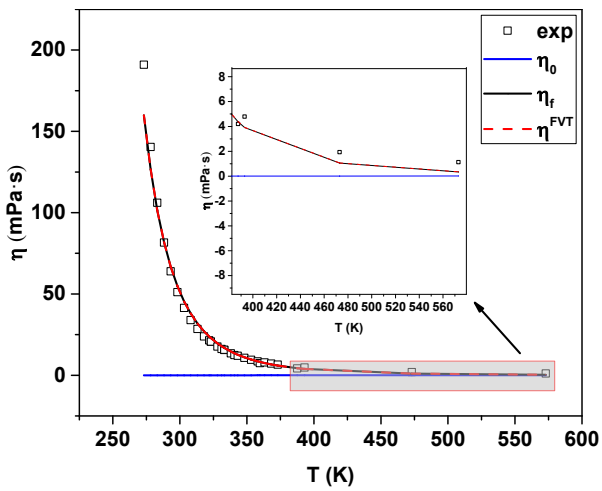

Figure 5. Viscosities of [BMIm][Tf_2N] at 100 kPa and different temperatures. (Symbols, experimental data; Blue solid line, black solid line and dash red line are dilute gas viscosity, residual friction viscosity and total viscosity of FVT model,

respectively.)

3.4. Comparison with previous models.

The models for calculating the viscosities of ILs at different temperatures and pressures are summarized in Table 2. It is shown that the framework that simultaneously combines transport and thermodynamic models is the most employed one. The FVT and FT models are more used to combine with thermodynamic models. Among these models, our FCCS-FVT method shows satisfactory accuracy and needs only 3 adjustable parameters. For the FVT based models, FCCS-FVT method shows higher accuracy than the simple cubic EoSs (PR and SRK equations) and comparable accuracy with more sophisticated EoSs (CPA and SAFT-based equations). For the other models with same framework, similar accuracy is found with our method. For example, the overall *AARDs* of FT+ePC-SAFT, MYS+SAFT-VR-Mie, and Eyring+GC are 1.39%, 2.37%, and 1.92%, respectively. However, most of them either need more parameters or adopt complicated mathematical formulas, which is inconvenient to implement. The deviations of the QSPR models are comparable with that from our method, but these QSPR models need professional software (e.g., HyperChem and COSMOthermX) to generate the descriptors, which limits their applications to an extent. The GC-FFANN method can be applied for large set of ILs, but the deviation from GC-FFANN method is larger than that from our FCCS-FVT method (11.42% vs. 6.6%). In summary, the developed FCCS-FVT method is an effective and accurate model to describe the $P\eta T$ behaviors of ILs. More importantly, their concise mathematical formulas make it easy to be used and extended. The concise strategy and mathematical formulas will enable it possible to be applied to others ILs when the data are available. Furthermore, the results from concise expressions can be transmitted to others commercial software (e.g., Aspen Plus and Fluent) by coding. It provides an opportunity to integrate the FCCS-FVT model into different scale studies, such as computational fluid dynamics simulations, process simulations, and so on.

FCCS-FVT method could be considered as a complimentary method rather than a replacement of existing models. Generally, each model has its own merits. The

theoretical methods have ability to extrapolate, such as FVT/FT-based methods, Eyring-based methods. The FT-based methods are usually superior to FVT-based methods for describing the relationship between viscosity and pressure.[16] Eyring-based methods can describe the $P\eta T$ behaviors of ILs well in their whole coverage of temperature and pressure because the maximum deviation of these models is less than 15%.[19] The correlation models, such as MYS-based models, are capable to describe the $P\eta T$ behaviors of ILs well in their whole coverage of temperature and pressure. MYS-based models are superior to FVT/FT-based models to describe the relationship between viscosity and pressure, especially at low pressure.[18] The QSPR models usually show predictive ability for new ILs. The GC-FFANN model is able to be applied at high pressure (such as > 300 MPa) because it has been developed with a wider coverage of pressure than that of other models.

Table 2. Summary of the models applicable at different temperatures and pressures

Model	N_{IL}	N_p	N_{par}	T range (K)	P range (MPa)	*AARD* (%)	Refs.
FVT+PR	9	583	3	273.15–353.15	0.1–300	16.62	15
FVT+SRK	9	583	3	273.15–353.15	0.1–300	18.70	
FVT+CPA	9	583	3	273.15–353.15	0.1–300	5.05	
FVT+PC-SAFT	9	583	3	273.15–353.15	0.1–300	3.75	
FT+PR	9	583	12	273.15–353.15	0.1–300	4.40	
FT+SRK	9	583	12	273.15–353.15	0.1–300	4.60	
FT+CPA	9	583	12	273.15–353.15	0.1–300	3.12	
FT+PC-SAFT	9	583	12	273.15–353.15	0.1–300	2.37	
FT+ePC-SAFT	9	604	12	273.15–353.15	0.1–300	1.39	16
FVT+ePC-SAFT	9	604	3	273.15–353.15	0.1–300	4.58	
FVT+soft-SAFT	6	—	3	283–636	0.1–300	5.13–9.11	17
FT+SAFT-VR-Mie	11	822	5	365 (Tmax)	300 (Pmax)	4.85	18
FVT+SAFT-VR-Mie	11	822	5	365 (Tmax)	300 (Pmax)	3.81	
MYS+SAFT-VR-Mie	11	822	3	365 (Tmax)	300 (Pmax)	2.37	
MYS + GSAFT-Cubic	11	822	3	365 (Tmax)	300 (Pmax)	4.04	
Eyring+PR	25	1070	5	273.15–433.15	0.06–300	2.03	19
Eyring+SRK	25	1070	5	273.15–433.15	0.06–300	2.01	
Eyring+GC	25	1070	5	273.15–433.15	0.06–300	1.92	
QSPR	349	3228	4	253.15–573.00	0.06–300	4.62	75
QSPR	89	1502	7	253.15–395.32	0.1–300	6.58	76

GC-FFANN	1484	over 13000	242	253–573	0.06–350	11.42	77
FCCS-FVT	25	2138	3	258.15–573	0.06–300	6.6	This work

* N_{IL} is the number of ILs; N_p is the number of data points; N_{par} is the number of parameters; QSPR: quantitative structure property relationship; GC: group contribution; MYS: modified Yarranton–Satyro correlation; FFANN: feed-forward artificial neural network.

4. CONCLUSIONS

In this study, fragment contribution corresponding states method (FCCS) is combined with free volume theory (FVT), named FCCS-FVT, to calculate the viscosities of ionic liquids (ILs) covering a wide range of temperatures (258.15−573 K) and pressures (0.06–300 MPa). The FCCS method is responsible for providing the critical properties and densities of ILs, which are subsequently used by the FVT method to calculate viscosities at given conditions. The results indicate that the FCCS-FVT method shows high accuracy with average absolute relative deviation and squared correlation coefficient being 6.6% and 0.965, respectively, for total 2138 data points of 25 ILs. On the other hand, only three parameters are required for FCCS-FVT method. The dilute gas viscosity item shows negligible contribution to the total viscosity of IL, indicating that FVT can be expressed with simpler mathematical formulas by ignoring the dilute gas viscosity item. In summary, the strategy of combining FCCS and FVT models is powerful to calculate viscosities of ILs due to its high accuracy and less parameters.

Supporting information

The experimental data details (including $P\eta T$ data, reference, and data set flag) of ILs and the corresponding calculated results (including η^{cal}, *RD, ARD, MSE,* R^2, *AARD*) from FCCS-FVT are summarized in Table S1−S25. The molecular weight, critical properties, acentric factor and the optimized parameters of each IL are reported in Table S26. The *MSE*, *AARD* and R^2 of each IL and entire data set for FCCS-FVT are

summarized in Table S27.

AUTHOR INFORMATION

Corresponding Authors

Dr. Shaojuan Zeng

Tel.: +86 01082544875 E-mail: sjzeng@ipe.ac.cn

Dr. Xiangping Zhang

Tel.: +86 01062558174 E-mail: xpzhang@ipe.ac.cn

ORCID

Shaojuan Zeng: 0000-0002-0070-6711

Xiaochun Zhang: 0000-0002-6691-0459

Xuezhong He: 0000-0002-3232-4945

Lei Liu: 0000-0001-8850-5553

Suojiang Zhang: 0000-0002-9397-954X

Xiangping Zhang: 0000-0002-1431-0873

Notes

The authors declare no competing financial interest.

ACKNOWLEDGEMENTS

This work is financially supported by the National Key R&D Program of China (2017YFB0603301), the Key Program of National Natural Science Foundation of China (21838010), the National Natural Scientific Foundation of China (U1704251, 21676271, 21890764), the DNL Cooperation Fund, CAS (DNL 180406), and the Research Council of Norway (CO2Hing, 267615).

Appendix A. full names and abbreviations of ionic liquids

[(2,3-M)BIm][Tf_2N]: 1-butyl-2,3-dimethyl-1H-imidazolium bis[(trifluoromethyl)sulfonyl]imide

[BMIm][BF_4]: 1-butyl-3-methylimidazolium tetrafluoroborate

[BMIm][PF_6]: 1-butyl-3-methylimidazolium hexafluorophosphate

[BMIm][Tf_2N]: 1-butyl-3-methylimidazolium bis[(trifluoromethyl)sulfonyl]imide

[BMPyr][CF_3SO_3]: 1-butyl-1-methylpyrrolidinium trifluoromethanesulfonate

[BMPyr][Tf_2N]: 1-butyl-1-methylpyrrolidinium bis[(trifluoromethyl)sulfonyl]imide

[BPy][BF_4]: 1-butylpyridinium tetrafluoroborate

[BPy][CF_3SO_3]: 1-butylpyridinium trifluoromethanesulfonate

[C_{10}MIm][Tf_2N]: 1-decyl-3-methylimidazolium bis[(trifluoromethyl)sulfonyl]imide

[C_3Py][BF_4]: 1-propylpyridinium tetrafluoroborate

[C_4(2-M)Py][BF_4]: 1-butyl-2-methylpyridinium tetrafluoroborate

[C_4(3-M)Py][BF_4]: 1-butyl-3-methylpyridinium tetrafluoroborate

[C_4(3-M)Py][Dca]: 1-butyl-3-methylpyridinium dicyanamide

[C_4(4-M)Py][BF_4]: 1-butyl-4-methylpyridinium tetrafluoroborate

[C_6MIm][BF_4]: 1-hexyl-3-methylimidazolium tetrafluoroborate

[C_6MIm][PF_6]: 1-hexyl-3-methylimidazolium hexafluorophosphate

[C_6MIm][Tf_2N]: 1-hexyl-3-methylimidazolium bis[(trifluoromethyl)sulfonyl]imide

[C_8(3-M)Py][BF_4]: N-octyl-3-methylpyridinium tetrafluoroborate

[C_8MIm][BF_4]: 1-octyl-3-methylimidazolium tetrafluoroborate

[C_8MIm][PF_6]: 1-octyl-3-methylimidazolium hexafluorophosphate

[DMIm][$MeSO_4$]: 1,3-dimethylimidazolium methylsulfate

[EMIm][BF_4]: 1-ethyl-3-methylimidazolium tetrafluoroborate

[EMIm][$EtSO_4$]: 1-ethyl-3-methylimidazolium ethyl sulfate

[EMIm][Tf_2N]: 1-ethyl-3-methylimidazolium bis[(trifluoromethyl)sulfonyl]imide

[(MoE)Mpyr][Tf_2N]: 1-(2-methoxyethyl)-1-methylpyrrolidinium bis[(trifluoromethyl)sulfonyl]imide

REFERENCES

(1) Dong, K.; Liu, X. M.; Dong, H. F.; Zhang, X. P.; Zhang, S. J. Multiscale Studies on Ionic Liquids. *Chem. Rev.* **2017,** 117, 6636-6695.

(2) Zeng, S. J.; Zhang, X. P.; Bai, L. P.; Zhang, X. C.; Wang, H.; Wang, J. J.; Bao, D.; Li, M. D.; Liu, X. Y.; Zhang, S. J. Ionic-Liquid-Based CO_2 Capture Systems: Structure, Interaction and Process. *Chem. Rev.* **2017,** 117, 9625-9673.

(3) Panda, S.; Gardas, R. L. Measurement and correlation for the thermophysical properties of novel pyrrolidonium ionic liquids: Effect of temperature and alkyl chain length on anion. *Fluid Phase Equilibr.* **2015,** 386, 65-74.

(4) Ziyada, A. K.; Wilfred, C. D. Effect of Temperature and Anion on Densities, Viscosities, and Refractive Indices of 1-Octyl-3-propanenitrile Imidazolium-Based Ionic Liquids. *J. Chem. Eng. Data* **2014,** 59, 1385-1390.

(5) Rogers, R. D.; Seddon, K. R. Ionic liquids - Solvents of the future? *Science* **2003,** 302, 792-793.

(6) Dai, Z.; Usman, M.; Hillestad, M.; Deng, L. Modelling of a tubular membrane contactor for pre-combustion CO_2 capture using ionic liquids: Influence of the membrane configuration, absorbent properties and operation parameters. *Green Energy Environ.* **2016,** 1, 266-275.

(7) Bandres, I.; Alcalde, R.; Lafuente, C.; Atilhan, M.; Aparicio, S. On the Viscosity of Pyridinium Based Ionic Liquids: An Experimental and Computational Study. *J. Phys. Chem. B* **2011,** 115, 12499-12513.

(8) Coutinho, J. A. P.; Carvalho, P. J.; Oliveira, N. M. C. Predictive methods for the estimation of thermophysical properties of ionic liquids. *Rsc Adv.* **2012,** 2, 7322-7346.

(9) Zhao, Y. S.; Zhang, X. P.; Deng, L. Y.; Zhang, S. J. Prediction of viscosity of imidazolium-based ionic liquids using MLR and SVM algorithms. *Comput. Chem. Eng.* **2016,** 92, 37-42.

(10) Alcalde, R.; García, G.; Atilhan, M.; Aparicio, S. Systematic Study on the Viscosity of Ionic Liquids: Measurement and Prediction. *Ind. Eng. Chem. Res.* **2015,** 54, 10918-10924.

(11) Sattari, M.; Kamari, A.; Hashemi, H.; Mohammadi, A. H.; Ramjugernath, D. A group contribution model for prediction of the viscosity with temperature dependency for fluorine-containing ionic liquids. *J. Fluorine Chem.* **2016,** 186, 19-27.

(12) Das, S.; Ojha, P. K.; Roy, K. Development of a temperature dependent 2D-QSPR

model for viscosity of diverse functional ionic liquids. *J. Mol. Liq.* **2017,** 240, 454-467.

(13) Mehrkesh, A.; Karunanithi, A. T. New quantum chemistry-based descriptors for better prediction of melting point and viscosity of ionic liquids. *Fluid Phase Equilibr.* **2016,** 427, 498-503.

(14) Zhang, Y.; Maginn, E. J. Direct Correlation between Ionic Liquid Transport Properties and Ion Pair Lifetimes: A Molecular Dynamics Study. *J. Phys. Chem. Lett.* **2015,** 6, 700-5.

(15) Haghbakhsh, R.; Parvaneh, K.; Shariati, A. Viscosities of Pure Ionic Liquids Using Combinations of Free Volume Theory or Friction Theory with the Cubic, the Cubic Plus Association, and the Perturbed-Chain Statistical Associating Fluid Theory Equations of State at High Pressures. *Ind. Eng. Chem. Res.* **2017,** 56, 2247-2258.

(16) Shen, G.; Held, C.; Mikkola, J.-P.; Lu, X.; Ji, X. Modeling the Viscosity of Ionic Liquids with the Electrolyte Perturbed-Chain Statistical Association Fluid Theory. *Ind. Eng. Chem. Res.* **2014,** 53, 20258-20268.

(17) Llovell, F.; Vega, L. F. Assessing Ionic Liquids Experimental Data Using Molecular Modeling: [$C_n$mim][BF_4] Case Study. *J. Chem. Eng. Data* **2014,** 59, 3220-3231.

(18) Abolala, M.; Peyvandi, K.; Varaminian, F. Modeling the viscosity of pure imidazolium-based ionic liquids using SAFT-VR-Mie EoS. *Fluid Phase Equilibr.* **2015,** 394, 61-70.

(19) He, M.; Zhu, C.; Liu, X. Estimating the viscosity of ionic liquid at high pressure using Eyring's absolute rate theory. *Fluid Phase Equilibr.* **2018,** 458, 170-176.

(20) Quinones-Cisneros, S. E.; Zeberg-Mikkelsen, C. K.; Stenby, E. H. The friction theory (f-theory) for viscosity modeling. *Fluid Phase Equilibr.* **2000,** 169, 249-276.

(21) Allal, A.; Boned, C.; Baylaucq, A. Free-volume viscosity model for fluids in the dense and gaseous states. *Phys. Rev. E* **2001,** 64.

(22) Huang, Y.; Dong, H. F.; Zhang, X. P.; Li, C. S.; Zhang, S. J. A new fragment contribution-corresponding states method for physicochemical properties prediction of ionic liquids. *AIChE J.* **2013,** 59, 1348-1359.

(23) Bao, D.; Zhang, X.; Dong, H.; Ouyang, Z.; Zhang, X.; Zhang, S. Numerical

simulations of bubble behavior and mass transfer in CO_2 capture system with ionic liquids. *Chem. Eng. Sci.* **2015,** 135, 76-88.

(24) Riedel, L. Liquid density in the saturated state. extension of the theorem of corresponding states II. *Chem. Ing. Tech.* **1954,** 26, 6.

(25) Kazakov, A.; Magee, J. W.; Chirico, R. D.; Paulechka, E.; Diky, V.; Muzny, C. D.; Kroenlein, K.; Frenkel, M. Version 2.0. NIST Standard Reference Database 147: NIST Ionic Liquids Database - (ILThermo). In National Institute of Standards and Technology: Gaithersburg MD, 2010.

(26) Gacino, F. M.; Paredes, X.; Comunas, M. J. P.; Fernandez, J. Pressure dependence on the viscosities of 1-butyl-2,3-dimethylimidazolium bis(trifluoromethylsulfonyl)imide and two tris(pentafluoroethyl)trifluorophosphate based ionic liquids: New measurements and modelling. *J. Chem. Thermodyn.* **2013,** 62, 162-169.

(27) Gacino, F. M.; Regueira, T.; Lugo, L.; Comunas, M. J. P.; Fernandez, J. Influence of Molecular Structure on Densities and Viscosities of Several Ionic Liquids. *J. Chem. Eng. Data* **2011,** 56, 4984-4999.

(28) Atilhan, M.; Jacquemin, J.; Rooney, D.; Khraisheh, M.; Aparicio, S. Viscous Behavior of Imidazolium-Based Ionic Liquids. *Ind. Eng. Chem. Res.* **2013,** 52, 16774-16785.

(29) Harris, K. R.; Kanakubo, M.; Woolf, L. A. Temperature and pressure dependence of the viscosity of the ionic liquid 1-butyl-3-methylimidazolium tetrafluoroborate: Viscosity and density relationships in ionic liquids. *J. Chem. Eng. Data* **2007,** 52, 2425-2430.

(30) Jacquemin, J.; Husson, P.; Padua, A. A. H.; Majer, V. Density and viscosity of several pure and water-saturated ionic liquids. *Green Chem.* **2006,** 8, 172-180.

(31) Neves, C. M. S. S.; Kurnia, K. A.; Coutinho, J. A. P.; Marrucho, I. M.; Lopes, J. N. C.; Freire, M. G.; Rebelo, L. P. N. Systematic Study of the Thermophysical Properties of Imidazolium-Based Ionic Liquids with Cyano-Functionalized Anions. *J. Phys. Chem. B* **2013,** 117, 10271-10283.

(32) Salgado, J.; Regueira, T.; Lugo, L.; Vijande, J.; Fernandez, J.; Garcia, J. Density

and viscosity of three (2,2,2-trifluoroethanol+1-butyl-3-methylimidazolium) ionic liquid binary systems. *J. Chem. Thermodyn.* **2014,** 70, 101-110.

(33) Sanmamed, Y. A.; Gonzalez-Salgado, D.; Troncoso, J.; Romani, L.; Baylaucq, A.; Boned, C. Experimental methodology for precise determination of density of RTILs as a function of temperature and pressure using vibrating tube densimeters. *J. Chem. Thermodyn.* **2010,** 42, 553-563.

(34) Tomida, D.; Kumagai, A.; Qiao, K.; Yokoyama, C. Viscosity of [bmim][PF_6] and [bmim][BF_4] at high pressure. *Int. J. Thermophys.* **2006,** 27, 39-47.

(35) Ahosseini, A.; Scurto, A. M. Viscosity of Imidazolium-Based Ionic Liquids at Elevated Pressures: Cation and Anion Effects. *Int. J. Thermophys.* **2008,** 29, 1222-1243.

(36) Bennett, V.; Dikio, C. W.; Angaye, S. S.; Wankasi, D.; Dikio, E. D.; Bahadur, I.; Ebenso, E. E. Interactions of 1-butyl-3-methylimidazolium hexafluorophosphate with N,N-dimethylformamide: Density and viscosity measurements. *J. Mol. Liq.* **2016,** 219, 661-666.

(37) Harris, K. R.; Woolf, L. A.; Kanakubo, M. Temperature and pressure dependence of the viscosity of the ionic liquid 1-butyl-3-methylimidazolium hexaftuorophosphate. *J. Chem. Eng. Data* **2005,** 50, 1777-1782.

(38) Zhu, J. Q.; Chen, J.; Li, C. Y.; Fei, W. Y. Viscosities and interfacial properties of 1-methyl-3-butylimidazolium hexafluorophosphate and 1-isobutenyl-3-methylimidazolium tetrafluoroborate ionic liquids. *J. Chem. Eng. Data* **2007,** 52, 812-816.

(39) Qiao, Y.; Yan, F. Y.; Xia, S. Q.; Yin, S.; Ma, P. S. Densities and Viscosities of [Bmim][PF_6] and Binary Systems [Bmim][PF_6] plus Ethanol, [Bmim][PF_6] plus Benzene at Several Temperatures and Pressures: Determined by the Falling-Ball Method. *J. Chem. Eng. Data* **2011,** 56, 2379-2385.

(40) Tomida, D.; Kumagai, A.; Qiao, K.; Yokoyama, C. Viscosity of 1-butyl-3-methylimidazolium hexafluorophosphate plus CO_2 mixture. *J. Chem. Eng. Data* **2007,** 52, 1638-1640.

(41) Harris, K. R.; Kanakubo, M.; Woolf, L. A. Temperature and pressure dependence of the viscosity of the ionic liquids 1-hexyl-3-methylimidazolium hexafluorophosphate

and 1-butyl-3-methylimidazolium bis(trifluoromethylsulfonyl)imide. *J. Chem. Eng. Data* **2007,** 52, 1080-1085.

(42) Liu, H. J.; Maginn, E.; Visser, A. E.; Bridges, N. J.; Fox, E. B. Thermal and Transport Properties of Six Ionic Liquids: An Experimental and Molecular Dynamics Study. *Ind. Eng. Chem. Res.* **2012,** 51, 7242-7254.

(43) Tariq, M.; Carvalho, P. J.; Coutinho, J. A. P.; Marrucho, I. M.; Lopes, J. N. C.; Rebelo, L. P. N. Viscosity of (C_2–C_{14}) 1-alkyl-3-methylimidazolium bis(trifluoromethylsulfonyl)amide ionic liquids in an extended temperature range. *Fluid Phase Equilibr.* **2011,** 301, 22-32.

(44) Gacino, F. M.; Comunas, M. J. P.; Regueira, T.; Segovia, J. J.; Fernandez, J. On the viscosity of two 1-butyl-1-methylpyrrolidinium ionic liquids: Effect of the temperature and pressure. *J. Chem. Thermodyn.* **2015,** 87, 43-51.

(45) Harris, K. R.; Woolf, L. A.; Kanakubo, M.; Ruther, T. Transport Properties of N-Butyl-N-methylpyrrolidinium Bis(trifluoromethylsulfonyl)amide. *J. Chem. Eng. Data* **2011,** 56, 4672-4685.

(46) Gacino, F. M.; Paredes, X.; Comunas, M. J. P.; Fernandez, J. Effect of the pressure on the viscosities of ionic liquids: Experimental values for 1-ethyl-3-methylimidazolium ethylsulfate and two bis(trifluoromethyl-sulfonyl)imide salts. *J. Chem. Thermodyn.* **2012,** 54, 302-309.

(47) Bandres, I.; Royo, F. M.; Gascon, I.; Castro, M.; Lafuente, C. Anion Influence on Thermophysical Properties of Ionic Liquids: 1-Butylpyridinium Tetrafluoroborate and 1-Butylpyridinium Triflate. *J. Phys. Chem. B* **2010,** 114, 3601-3607.

(48) Larriba, M.; Garcia, S.; Navarro, P.; Garcia, J.; Rodriguez, F. Physical Properties of N-Butylpyridinium Tetrafluoroborate and N-Butylpyridinium Bis(trifluoromethylsulfonyl)imide Binary Ionic Liquid Mixtures. *J. Chem. Eng. Data* **2012,** 57, 1318-1325.

(49) Mokhtarani, B.; Sharifi, A.; Mortaheb, H. R.; Mirzaei, M.; Mafi, M.; Sadeghian, F. Density and viscosity of pyridinium-based ionic liquids and their binary mixtures with water at several temperatures. *J. Chem. Thermodyn.* **2009,** 41, 323-329.

(50) Bandres, I.; Lopez, M. C.; Castro, M.; Barbera, J.; Lafuente, C. Thermophysical

properties of 1-propylpyridinium tetrafluoroborate. *J. Chem. Thermodyn.* **2012,** 44, 148-153.

(51) Bandres, I.; Pera, G.; Martin, S.; Castro, M.; Lafuente, C. Thermophysical Study of 1-Butyl-2-Methylpyridinium Tetrafluoroborate Ionic Liquid. *J. Phys. Chem. B* **2009,** 113, 11936-11942.

(52) Bandres, I.; Giner, B.; Artigas, H.; Royo, F. M.; Lafuente, C. Thermophysic comparative study of two isomeric pyridinium-based ionic liquids. *J. Phys. Chem. B* **2008,** 112, 3077-3084.

(53) Crosthwaite, J. M.; Muldoon, M. J.; Dixon, J. K.; Anderson, J. L.; Brennecke, J. F. Phase transition and decomposition temperatures, heat capacities and viscosities of pyridinium ionic liquids. *J. Chem. Thermodyn.* **2005,** 37, 559-568.

(54) Bandres, I.; Giner, B.; Gascon, I.; Castro, M.; Lafuente, C. Physicochemical characterization of n-butyl-3-methylpyridinium dicyanamide ionic liquid. *J. Phys. Chem. B* **2008,** 112, 12461-12467.

(55) Hernandez-Galvan, M. A.; Garcia-Sanchez, F.; Garcia-Flores, B. E.; Castro-Arellano, J. Liquid Viscosities of Cyclohexane, Cyclohexane plus Tetradecane, and Cyclohexane plus Benzene from (313 to 393) K and Pressures Up to 60 MPa. *J. Chem. Eng. Data* **2009,** 54, 2831-2838.

(56) Shiflett, M. B.; Elliott, B. A.; Yokozeki, A. Phase behavior of vinyl fluoride in room-temperature ionic liquids [emim][Tf_2N], [bmim][$N(CN)_2$], [bmpy][BF_4], [bmim][HFPS] and [omim][TFES]. *Fluid Phase Equilibr.* **2012,** 316, 147-155.

(57) Beigi, A. A. M.; Abdouss, M.; Yousefi, M.; Pourmortazavi, S. M.; Vahid, A. Investigation on physical and electrochemical properties of three imidazolium based ionic liquids (1-hexyl-3-methylimidazolium tetrafluoroborate, 1-ethyl-3-methylimidazolium bis(trifluoromethylsulfonyl) imide and 1-butyl-3-methylimidazolium methylsulfate). *J. Mol. Liq.* **2013,** 177, 361-368.

(58) Sanmamed, Y. A.; Gonzalez-Salgado, D.; Troncoso, J.; Cerdeirina, C. A.; Romani, L. Viscosity-induced errors in the density determination of room temperature ionic liquids using vibrating tube densitometry. *Fluid Phase Equilibr.* **2007,** 252, 96-102.

(59) Song, D. Y.; Chen, J. Density and Viscosity Data for Mixtures of Ionic Liquids with a Common Anion. *J. Chem. Eng. Data* **2014,** 59, 257-262.

(60) Tomida, D.; Kenmochi, S.; Tsukada, T.; Qiao, K.; Bao, Q. X.; Yokoyama, C. Viscosity and Thermal Conductivity of 1-Hexyl-3-methylimidazolium Tetrafluoroborate and 1-Octyl-3-methylimidazolium Tetrafluoroborate at Pressures up to 20 MPa. *Int. J. Thermophys.* **2012,** 33, 959-969.

(61) Tomida, D.; Kumagai, A.; Kenmochi, S.; Qiao, K.; Yokoyama, C. Viscosity of 1-hexyl-3-methylimidazolium hexafluorophosphate and 1-octyl-3-methylimidazolium hexafluorophosphate at high pressure. *J. Chem. Eng. Data* **2007,** 52, 577-579.

(62) Vakili-Nezhaad, G.; Vatani, M.; Asghari, M.; Ashour, I. Effect of temperature on the physical properties of 1-butyl-3-methylimidazolium based ionic liquids with thiocyanate and tetrafluoroborate anions, and 1-hexyl-3-methylimidazolium with tetrafluoroborate and hexafluorophosphate anions. *J. Chem. Thermodyn.* **2012,** 54, 148-154.

(63) Kandil, M. E.; Marsh, K. N.; Goodwin, A. R. H. Measurement of the viscosity, density, and electrical conductivity of 1-hexyl-3-methylimidazolium bis(trifluorosulfonyl)imide at temperatures between (288 and 433) K and pressures below 50 MPa. *J. Chem. Eng. Data* **2007,** 52, 2382-2387.

(64) Nazet, A.; Sokolov, S.; Sonnleitner, T.; Makino, T.; Kanakubo, M.; Buchner, R. Densities, Viscosities, and Conductivities of the Imidazolium Ionic Liquids [Emim][Ac], [Emim][FAP], [Bmim][BETI], [Bmim][FSI], [Hmim][TFSI], and [Omim][TFSI]. *J. Chem. Eng. Data* **2015,** 60, 2400-2411.

(65) Widegren, J. A.; Magee, J. W. Density, viscosity, speed of sound, and electrolytic conductivity for the ionic liquid 1-hexyl-3-methylimidazolium bis(trifluoromethylsulfonyl)imide and its mixtures with water. *J. Chem. Eng. Data* **2007,** 52, 2331-2338.

(66) Harris, K. R.; Kanakubo, M.; Woolf, L. A. Temperature and pressure dependence of the viscosity of the ionic liquids 1-methyl-3-octylimidazolium hexafluorophosphate and 1-methyl-3-octylimidazolium tetrafluoroborate. *J. Chem. Eng. Data* **2006,** 51, 1161-1167.

(67) Mokhtarani, B.; Mojtahedi, M. M.; Mortaheb, H. R.; Mafi, M.; Yazdani, F.; Sadeghian, F. Densities, refractive indices, and viscosities of the ionic liquids 1-methyl-3-octylimidazolium tetrafluoroborate and 1-methyl-3-butylimidazolium perchlorate and their binary mixtures with ethanol at several temperatures. *J. Chem. Eng. Data* **2008,** 53, 677-682.

(68) Rocha, M. A. A.; Ribeiro, F. M. S.; Ferreira, A. I. M. C. L.; Coutinho, J. A. P.; Santos, L. M. N. B. F. Thermophysical properties of $[C_{N-1}C_1im][PF_6]$ ionic liquids. *J. Mol. Liq.* **2013,** 188, 196-202.

(69) AlTuwaim, M. S.; Alkhaldi, K. H. A. E.; Al-Jimaz, A. S.; Mohammad, A. A. Temperature Dependence of Physicochemical Properties of Imidazolium-, Pyroldinium-, and Phosphonium-Based Ionic Liquids. *J. Chem. Eng. Data* **2014,** 59, 1955-1963.

(70) Aparicio, S.; Alcalde, R.; Garcia, B.; Leal, J. M. High-Pressure Study of the Methylsulfate and Tosylate Imidazolium Ionic Liquids. *J. Phys. Chem. B* **2009,** 113, 5593-5606.

(71) Pereiro, A. B.; Santamarta, F.; Tojo, E.; Rodriguez, A.; Tojo, J. Temperature dependence of physical properties of ionic liquid 1,3-dimethylimidazolium methyl sulfate. *J. Chem. Eng. Data* **2006,** 51, 952-954.

(72) Schreiner, C.; Zugmann, S.; Hartl, R.; Gores, H. J. Fractional Walden Rule for Ionic Liquids: Examples from Recent Measurements and a Critique of the So-Called Ideal KCl Line for the Walden Plot. *J. Chem. Eng. Data* **2010,** 55, 1784-1788.

(73) Froba, A. P.; Kremer, H.; Leipertz, A. Density, refractive index, interfacial tension, and viscosity of ionic liquids $[EMIM][EtSO_4]$, $[EMIM][NTf_2]$, $[EMIM][N(CN)_2]$, and $[OMA][NTf_2]$ in dependence on temperature at atmospheric pressure. *J. Phys. Chem. B* **2008,** 112, 12420-12430.

(74) Hofmann, A.; Migeot, M.; Hanemann, T. Investigation of Binary Mixtures Containing 1-Ethyl-3-methylimidazolium Bis(trifluoromethanesulfonyl)azanide and Ethylene Carbonate. *J. Chem. Eng. Data* **2016,** 61, 114-123.

(75) Yan, F.; He, W.; Jia, Q.; Wang, Q.; Xia, S.; Ma, P. Prediction of ionic liquids viscosity at variable temperatures and pressures. *Chem. Eng. Sci.* **2018,** 184, 134-140.

(76) Zhao, Y.; Huang, Y.; Zhang, X.; Zhang, S. A quantitative prediction of the viscosity of ionic liquids using $S_{\sigma\text{-profile}}$ molecular descriptors. *Phys. Chem. Chem. Phys.* **2015,** 17, 3761-7.

(77) Paduszynski, K.; Domanska, U. Viscosity of ionic liquids: an extensive database and a new group contribution model based on a feed-forward artificial neural network. *J. Chem. Inf. Model.* **2014,** 54, 1311-24.

Graphic Abstract